Available online at www.sciencedirect.com
SCIENCE DIRECT®
Journal of Crystal Growth 289 (2006) 55–58
JOURNAL OF CRYSTAL GROWTH
www.elsevier.com/locate/jcrysgro

# Photoluminescence and Raman behaviors of ZnO nanostructures with different morphologies

S.J. Chen[a,b,c], Y.C. Liu[c,*], Y.M. Lu[a], J.Y. Zhang[a], D.Z. Shen[a], X.W. Fan[a]

[a]*Key Laboratory of Excited State Process, Changchun Institute of Optics, Fine Mechanics and Physics, Chinese Academy of Sciences, 16 East South Lake Avenue, Changchun 130021, People's Republic of China*
[b]*Graduate School of the Chinese Academy of Sciences, Beijing 100049, People's Republic of China*
[c]*Centre for Advanced Optoelectronic Functional Material Research, Northeast Normal University, Changchun 130024, People's Republic of China*

Received 1 December 2004; received in revised form 21 May 2005; accepted 13 October 2005
Available online 22 December 2005
Communicated by R. James

**Abstract**

The morphology, structure and photoluminescence properties of ZnO nanostructures synthesized from different zinc precursors by a vapor transport process were investigated. The zinc precursors involved pure zinc powder, zinc powder mixed with graphite and zinc powder mixed with carbon nanotubes. The products were characterized by XRD, FESEM, TEM, Raman and PL techniques. The results indicated that the zinc precursors have a strong effect on the morphology and structural properties of the ZnO nanostructures. For the pure zinc, zinc mixed with graphite and zinc mixed with carbon nanotube, uniform tetrapod-, chrysanthemum- and needle-like morphologies are obtained, respectively. Photoluminescence measurements show that all the products have a strong near-band-edge UV emission accompanied by weak visible emissions. The relatively stronger green-light emission from the tetrapods implies that more defects exist in the tetrapods. A peak at 445 nm is found in the spectrum of the tetrapod-like nanostructures, which may be caused by oxygen-depletion interface traps. Furthermore, products synthesized at 600 °C demonstrate better photoluminescence properties than those synthesized at 450 °C.


*Keywords:* A1. Photoluminescence; A1. Raman spectra; B1. ZnO nanostructures

## 1. Introduction

In recent years, nanosize semiconductors have attracted much attention, due to their special electrical and optical characteristics in fabricating nanoscaled electronic and optoelectronic devices. Among them, one-dimensional (1D) nanostructures such as nanotubes [1], nanowires [2], nanorods [3], nanobelts [4], nanocables [5], and nanoribbons [6] have stimulated considerable interest for scientific research due to their importance in fundamental physics studies and their potential applications in nanoelectronics, nanomechanics, and flat panel displays.

Zinc oxide (ZnO) is of much interest because of its attractive optical properties based on its wide band gap of 3.37 eV and exciton binding energy of 60 meV, which is larger than the thermal energy at room temperature. In this regard, ZnO is regarded as a promising photonic material for UV/blue devices, such as short-wavelength light-emitting diodes and laser diodes. A particularly striking recent observation is that of lasing action in micron-sized rods [2,7]. ZnO has been prepared by a number of methods such as the reaction of zinc salt with base [8–11], chemical bath deposition [12–14], thermal decomposition [15], hydrothermal synthesis [16], sol–gel methods [17–19], template methods including the use of alumina membranes [20], and vapor phase transport [2].

In this work, we fabricated ZnO nanostructures by a vapor transport process from pure zinc powder, zinc powder mixed with graphite and zinc powder mixed with carbon nanotube (CNT), respectively, in order to investigate the change in the shape, structure and optical properties of the obtained structures by varying the Zn precursors.

*Corresponding author. Tel.: +86 4315269168; fax: +86 4315684009.
*E-mail address:* ycliu@nenu.edu.cn (Y.C. Liu).

0022-0248/$ - see front matter © 2005 Elsevier B.V. All rights reserved.
doi:10.1016/j.jcrysgro.2005.10.137

## 2. Experiments

ZnO nanostructures were synthesized in a horizontal tube furnace by a vapor-deposition method. Zinc sources were chosen as pure zinc powder, zinc powder mixed with graphite (1:1) and zinc powder mixed with CNT (1:1), respectively. The evaporation process was carried out in quartz tubes, which were located in the horizontal tube furnace. Three clean quartz tubes loaded with the above-mentioned three Zn sources, respectively, were simultaneously inserted in a furnace at room temperature. Pure $O_2$ (5 N) was used to purge the air-tight tubes. The furnace was heated slowly to 450 °C and maintained for 2 h. After the system had been naturally cooled to room temperature, gray–white products were obtained. Another experiment was also done at similar conditions except at a temperature of 600 °C. The materials were collected and characterized using field-emission scanning electron microscopy (FESEM; S-4200), X-ray diffraction (XRD) and transmission electron microscopy (TEM). Raman spectra were measured with a JY HR800 microlaser Raman spectrometer with a backscattering optical configuration. An argon ion laser at 488 nm was used as the excitation source. PL measurements were carried out with a micro-PL system at temperatures from 80 to 857 K. A He–Cd laser at 325 nm was used for PL excitation.

## 3. Results and discussion

The morphologies of the products were observed by FE-SEM and TEM. The typical images synthesized at 450 °C are shown in Fig. 1. It can be observed that when pure Zn powder source is used (Fig. 1a), tetrapod-like structures with a large yield were obtained. Fig. 1b shows a TEM image of a typical single tetrapod. Unlike previously reported tetrapod structures [21], our obtained tetrapods were not uniform. In some areas of the sample, tricorn-cone structures are obtained. The tricon-cone structures are believed to come from tetrapods, as shown in Fig. 1a. When the metallic Zn and graphite (1:1) are used as starting materials (Fig. 1c,d), the ZnO nanocrystals have chrysanthemum-like morphologies, and the diameters range from 3 to 8 μm. It is interesting that a chrysanthemum-like ZnO nanostructure (Fig. 1d) is composed of a large quantity of small ZnO nanorods radial from a same center. When the metallic Zn and CNT (1:1) are used as starting materials (Fig. 1e, f), needle-like ZnO nanocrystals are obtained. The diameters of the needles are in the range of 10–50 nm and the length range from 1 to 3 μm. Also, the morphologies of the products synthesized at 600 °C were observed by FE-SEM and TEM. The typical images were almost the same as the images at 450 °C, respectively, except that they were larger.

The starting reagents have much influence on the morphologies of ZnO nanocrystals. ZnO nanocrystals of three different morphologies were obtained with similar experimental processes. ZnO tetrapod-like structures can

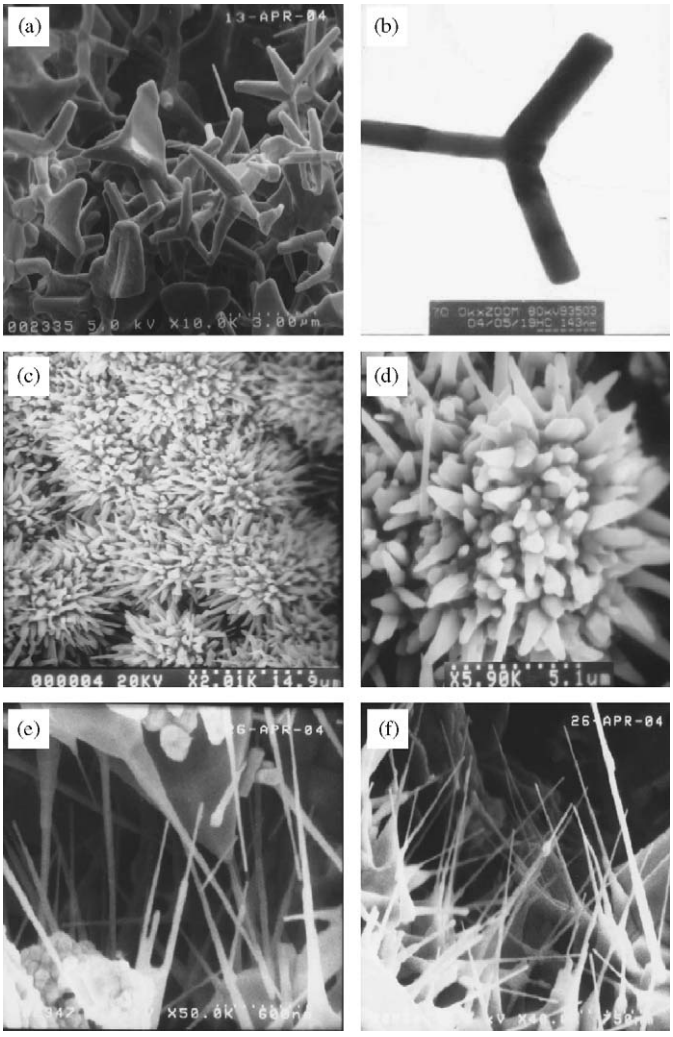


Fig. 1. (a) Low magnification of FESEM image of ZnO tetrapod-like structures, (b) TEM image of a typical single tetrapod, (c) low-magnification FESEM image of ZnO chrysanthemum-like morphologies, (d) higher magnification of FESEM image of a single chrysanthemum-like structure, (e) and (f) needle-like structures from Zn powder and CNT.

be obtained using pure Zn powder as the starting material. Growth of large tetrapod crystals was demonstrated previously [21,22]. Observation of ZnO tetrapod nanorods is similar to the result reported by Dai et al. [23]. There was no report of a tricorn-cone structure growing from tetrapod ZnO. In our work no catalyst was used, and the obtained results in air were similar to the result reported by Dai et al. [23]. Therefore, it is likely that the growth mechanism is vapor–solid.

When Zn and graphite were used as the starting materials, chrysanthemum-like ZnO nanocrystals were produced. Needle-like ZnO nanocrystals were obtained when CNT was used instead of graphite. In the two cases, we think that the graphite and CNT do not act as reactants to form ZnO nanostructures, but as templates guiding the growth of chrysanthemum-like and needle-like ZnO nanostructures, respectively. It is suggested that the choice of appropriate starting materials is very important for the synthesis of nanomaterials with novel morphologies.

Fig. 2 shows the Raman spectra of ZnO nanocrystals grown under 450 °C. As shown in Fig. 2, the three spectra have similar shapes. The peak at 437 $cm^{-1}$ corresponds to $E_2$ mode of ZnO crystal, and the peak at 330 $cm^{-1}$ should be assigned to the second order Raman spectrum arising from zone-boundary phonons $3E_{2H}$–$E_{2L}$, while the peak at 561 $cm^{-1}$ is a contribution of the $E_1$ (LO) mode of ZnO associated with oxygen deficiency [24]. Such a strong intensity of the $E_1$ mode indicates that the ZnO nanocrystals grown at 450 °C are severely oxygen deficient.

The Raman spectra of ZnO nanocrystals grown at 600 °C are shown in Fig. 3. Compared with the Raman spectra grown at 450 °C, three Raman spectra are stronger and there is a sharper $E_2$ mode and much lower $E_1$ (LO) mode. In addition, $A_{1T}$ and $E_{1T}$ modes could be observed in the spectra. The stronger $E_2$ mode and much lower $E_1$ (LO) mode indicate that a lower oxygen vacancy is present in the samples. The samples grown at higher temperature exhibit very low oxygen vacancy. Furthermore, tetrapod-like ZnO exhibits better Raman signal than chrysanthemum-like and needle-like ZnO, which possibly results from better crystal quality and less impurities due to the use of pure metallic Zn starting reagents.

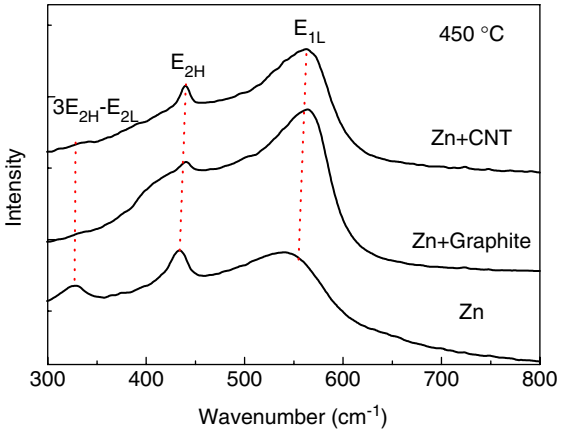


Fig. 2. Raman spectra of the ZnO nanostructures grown at 450 °C using an excitation wavelength at 488 nm.

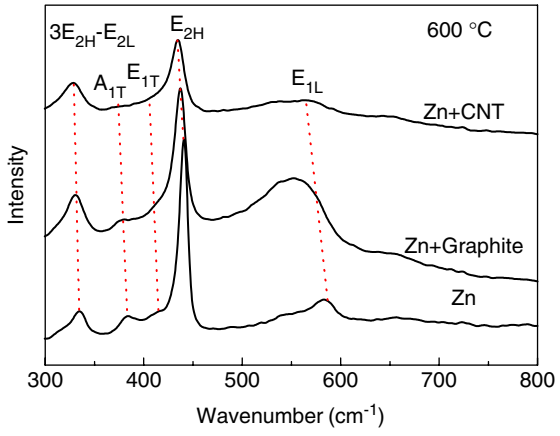


Fig. 3. Raman spectra of the ZnO nanostructures grown at 600 °C using an excitation wavelength at 488 nm.

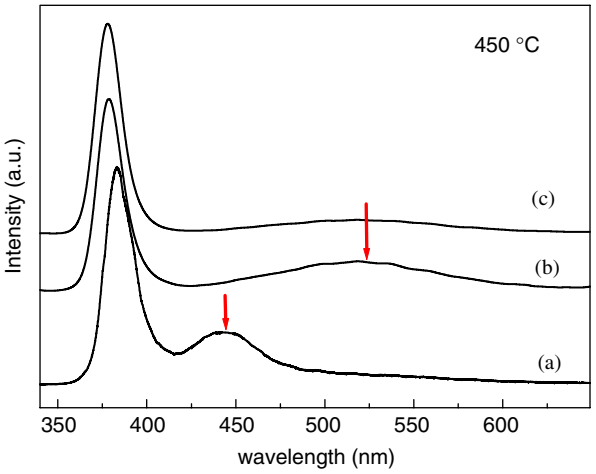


Fig. 4. PL spectra of the ZnO nanostructures grown at 450 °C measured at room temperature.

The PL spectra of ZnO nanocrystals with tetrapod-, chrysanthemum- and needle-like morphologies were measured at room temperature. Fig. 4 shows the PL spectra from the samples synthesized at 450 °C. All spectra have a strong UV emission at 390 nm and a relatively weak visible emission at 530 nm. The UV band emission of ZnO has been well demonstrated to be related to the exciton emission [25]. Although the mechanism of green emission in ZnO crystal has not been identified clearly, models related to various defects, which can provide the recombination centers within the band gap, have been suggested. A singly ionized oxygen vacancy has been reported to be responsible for the green emission in ZnO, and this emission results from the recombination of a photogenerated hole with the singly ionized charge state of this defect [26].

Fig. 4a–c shows that the green emission of chrysanthemum-like ZnO nanocrystals is stronger than the other samples. It is well known that surface states may significantly influence the PL process in nanomaterials and the progressive increase of the green light emission intensity relative to the UV emission is observed as the wire diameter decreases, which suggests that there is a large fraction of oxygen vacancies in the nanorods. Except for two-band fluorescence mentioned above, a new blue band at 445 nm was recorded in the tetrapod-like ZnO nanocrystals (in Fig. 4c). This peak was also found in ZnO nanorod arrays [27]. Jin et al. [28] considered it might be due to the existence of oxygen-depleted interface traps in $ZnO_x$. In contrast to the UV spectra, visible fluorescence spectra of ZnO were sensitive to the preparation processes, from which some new defects were created. When the graphite and CNT were used as starting reagents, graphite and CNT can produce C, so the new defects were probably caused by the combination of C and O. Further investigation of the PL properties of nanostructured ZnO is still needed.

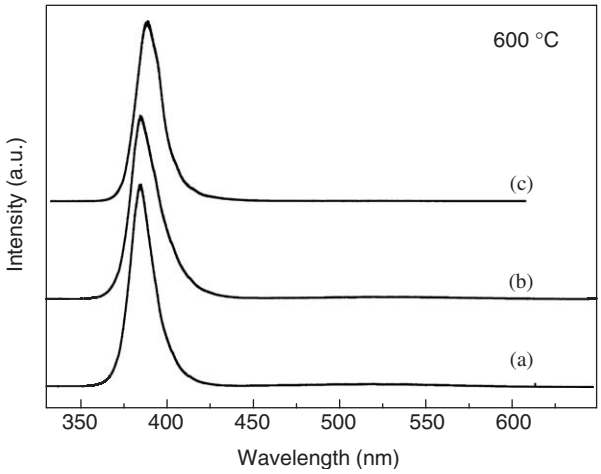


Fig. 5. PL spectra of the ZnO nanostructures grown at 600 °C measured at room temperature.

The PL spectra of ZnO nanostructure samples synthesized at 600 °C are shown in Fig. 5. In comparison with the PL spectra synthesized at 450 °C, the PL spectra show much weaker visible emission and sharper UV peak, which shows much better optical properties. The PL results are consistent with the Raman results.

## 4. Conclusions

Different morphologies of ZnO nanostructures such as uniform tetrapod-, chrysanthemum- and needle-like morphologies are obtained from pure zinc powder, zinc powder mixed with graphite and zinc powder mixed with CNT, respectively. FESEM and TEM results show the starting reagents have much influence on the morphologies of ZnO nanocrystals. Raman data show that all the products synthesized at 450 °C exhibit a strong intensity of the $E_1$ mode due to severe oxygen deficiency in the ZnO nanocrystals. For products synthesized at 600 °C, the oxygen deficiency was much reduced, which is confirmed by the PL results. PL results also indicate that the starting reagents and the temperature have much influence on the optical properties of ZnO nanocrystals.

## Acknowledgments

This work was supported by the National Natural Science Foundation of China, No. 60176003 and No. 60376009, and the Foundational Excellent Researcher to Go beyond Century of Ministry of Education of China. Science Foundation for Yong Teachers of Northeast Normal University, no. 20050202.

## References

[1] S. Iijima, Nature 354 (1991) 56.
[2] M.H. Huang, S. Mao, H. Feick, H. Yan, Y. Wu, H. Kind, et al., Science 292 (2001) 1897.
[3] J.Y. Li, X.L. Chen, H. Li, M. He, Z.Y. Qiao, J. Crystal Growth 233 (2001) 5.
[4] Z.W. Pan, Z.R. Dai, Z.L. Wang, Science 291 (2001) 1947.
[5] J. Wu, S. Liu, C. Wu, K. Chen, L. Chen, Appl. Phys. Lett. 81 (2002) 1312.
[6] B.D. Yao, Y.F. Chan, N. Wang, Appl. Phys. Lett. 81 (2002) 757.
[7] K. Govender, D.S. Boyle, P. O'Brien, D. Binks, D. West, D. Coleman, Adv. Mater. 14 (2002) 1221.
[8] S.M. Haile, D.W. Johnson, G.H. Wiseman, H.K. Bowen, J. Am. Ceram. Soc. 72 (2004) 1989.
[9] T. Trinidade, J.D.P. Dejesus, P. O'Brien, J. Mater. Chem. 4 (1994) 1615.
[10] A. Chittofrati, E. Matijevic, Colloid Surf. 48 (1990) 65.
[11] C. Pacholski, A. Kornowski, H. Weller, Angew. Chem. Int. Ed. 41 (2002) 1188.
[12] P. O'Brien, T. Saeed, J. Knowles, J. Mater. Chem. 6 (1996) 1135.
[13] L. Vayssieres, K. Keis, S.E. Lindquist, A. Hagfeldt, J. Phys. Chem. B 105 (2001) 3350.
[14] D.S. Boyle, K. Govender, P. O'Brien, Chem. Commun. 1 (2002) 80.
[15] N. Audebrand, J.P. Auffredic, D. Louer, Chem. Mater. 10 (1998) 2450.
[16] C.-H. Lu, C.-H. Yeh, Ceram. Int. 26 (2000) 351.
[17] S.-Y. Chu, T.-M. Yan, S.-L. Chen, J. Mater. Sci. Lett. 19 (2000) 349.
[18] C.L. Carnes, K.L. Klabunde, Langmuir 16 (2000) 3764.
[19] G. Westin, A. Ekstrand, M. Nygren, R. Osterlund, P. Merkelbach, J. Mater. Chem. 4 (1994) 615.
[20] Y.C. Wang, I.C. Leu, M.H. Hon, J. Mater. Chem. 12 (2002) 2439.
[21] W.D. Yu, X.M. Li, X.D. Gao, Chem. Phys. Lett. 390 (2004) 296.
[22] H.L. Yu, B.D. Aleksandra, G. Ju, H.X. Mao, K.C. Wai, Chem. Phys. Lett. 385 (2004) 155.
[23] Y. Dai, Y. Zhang, Q.K. Li, C.W. Nan, Chem. Phys. Lett. 358 (2002) 83.
[24] G.J. Exarhos, S.K. Sharma, Thin Solid Films 270 (1995) 27.
[25] L. Spanhel, M.A. Anderson, J. Am. Chem. Soc. 113 (1991) 2826.
[26] K. Vanheusden, W.L. Warren, C.H. Seager, D.R. Tallant, J.A. Voigt, J. Appl. Phys. 79 (1996) 7983.
[27] J.J. Wu, S.C. Liu, Adv. Mater. 14 (2002) 215.
[28] B.J. Jin, S. Im, S.Y. Lee, Thin Solid Films 366 (2000) 107.